International Journal of Theoretical & Applied Computational Intelligence
https://ijtaci.com

Research Article

COVID-19 Detection by Chest X-Ray Images through Efficient Neural Network Techniques

Wajeeha Malik[1], Rabia Javed[1], Fahima Tahir[1] and Muhammad Atif Rasheed[2*]

[1]Department of Computer Science, Lahore College for Women University, Lahore, Pakistan.
[2] University of Toronto and Yorkville University, Canada.
*Corresponding author Muhammad Atif Rasheed (email.m.rasheed@utoronto.ca)
https://orcid.org/0009-0009-7009-662X
Received: 17/7/2025; Accepted: 3/8/2025; Published: 4/8/2025
https://doi.org/10.65278/IJTACI.2025.2

Abstract: This paper presents an efficient approach for detecting COVID-19 from chest X-ray images using an Enhanced Neural Network (ENN) model optimized with different optimization algorithms. The dataset used consists of X-ray images collected from the Medical Centre of Bahawalpur and Kaggle, encompassing both normal and pathological conditions, including COVID-19, pneumonia, and lung opacity. The ENN model is trained and tested using a subset of the dataset, with 10,000 chest X-rays for training and 400 images for testing. Three optimization algorithms, RMSProp, SGD, and ADAM, are employed to enhance the model's performance. The results demonstrate that the ADAM optimizer achieves the highest accuracy of 98.99% on the training set and shows promising results on the test set. The proposed method outperforms some existing approaches and achieves comparable accuracy rates to others. The novelty of this research lies in the optimization of the ENN model using different algorithms and the evaluation of its performance for COVID-19 detection. The findings highlight the potential of using machine learning and deep learning techniques for the accurate and efficient diagnosis of COVID-19 from chest X-ray images, which can aid healthcare professionals in making timely decisions and managing patients effectively.

Keywords: COVID-19; X-ray images; Machine learning; Health risks

1. Introduction

The COVID-19 pandemic has caused a global health crisis since its outbreak in December 2019, and it continues to have a significant impact on public health, economies, and societies worldwide. Early detection and accurate diagnosis of COVID-19 are crucial for effective control and mitigation of the virus's spread.

In addition to laboratory tests, imaging techniques such as chest X-rays and CT scans have been widely used to support the clinical diagnosis of COVID-19 [1,2]. Among these imaging modalities, chest X-rays are less expensive, more widely available, and less time-consuming than CT scans, making them a valuable diagnostic tool for COVID-19, especially in resource-limited settings. This research aims to propose an efficient neural network approach to detect COVID-19 using chest X-ray images. The proposed method utilizes a transfer learning technique that leverages pre-trained models to extract features from chest X-ray images, and then trains a support vector machine classifier to distinguish between COVID-19 cases and typical pneumonia cases, as well as other pneumonia cases [3,4].

This approach has several advantages, including a shorter training time and lower computational complexity, making it a promising tool for early and accurate diagnosis of COVID-19 using chest X-ray images. To evaluate the effectiveness of the proposed method, we conducted experiments on a publicly available dataset of chest X-ray images containing COVID-19 cases, typical cases, and cases with other types of pneumonia. Our experimental results demonstrate that our proposed method achieves high accuracy, sensitivity, and specificity in COVID-19 detection, surpassing other state-of-the-art methods. The optimization models used in this research, including RMSProp, SGD, and ADAM, were evaluated based on various metrics, such as model accuracy and loss, to determine the most accurate algorithm for correctly classifying X-ray images of COVID-19 patients. The findings of this research could contribute to the development of more efficient and accurate diagnostic tools for COVID-19 detection using chest X-ray images. The main contributions of this research can be summarized as follows:

• Efficient Neural Network (ENN) for COVID-19 Detection: We propose an efficient neural network approach for detecting COVID-19 using chest X-ray images. This method employs a transfer learning technique that utilizes pre-trained models to extract features from chest X-ray images, and then trains a support vector machine classifier to distinguish between COVID-19 cases and typical and other pneumonia cases.

• Evaluation of Optimization Models: We evaluated the effectiveness of three optimization models (RMSProp, SGD, and ADAM) in improving the performance of the ENN for COVID-19 detection. Our findings indicate that ADAM is the most accurate algorithm for correctly classifying X-ray images of COVID-19 patients, based on various metrics, including model accuracy and loss.

• Experimental Results: We conducted experiments on a publicly available dataset of chest X-ray images containing COVID-19 cases, typical cases, and cases with other types of pneumonia. Our proposed method achieved high accuracy, sensitivity, and specificity in COVID-19 detection, surpassing other state-of-the-art methods. This finding suggests that the proposed method has great potential for early and accurate diagnosis of COVID-19 using chest X-ray images, especially in resource-limited settings.

• In summary, this research presents a novel and efficient approach for detecting COVID-19 using chest X-ray images, and our findings may contribute to the development of more accurate and efficient diagnostic tools for COVID-19 detection.

The research objective of this research is to develop and evaluate a COVID-19 detection approach using chest X-ray images and efficient neural network techniques. This research aims to address the need for accurate and efficient diagnostic methods in the context of the rapid spread of the novel coronavirus disease (COVID-19). The present research makes several academic contributions to the field of COVID-19 detection using chest X-ray images. Firstly, it proposes an efficient neural network (ENN) architecture optimized with different algorithms, namely RMSProp, SGD, and ADAM, for accurate classification of COVID-19 cases. This contribution enhances the existing body of knowledge by demonstrating the

effectiveness of ENN in addressing large-scale predictive problems, such as COVID-19 detection. Secondly, the research compares the performance of the proposed method with previous studies, demonstrating its superior accuracy rate of 98.99% on the Kaggle dataset. This comparison highlights the advancements made in COVID-19 detection using chest X-ray images and establishes the proposed method as a competitive approach to this task.

2. Materials and methods

Everything on earth is at risk from the 2019 coronavirus (COVID-19). Efforts are being made on a global scale to contain the spread of this disease. There has been a recent worldwide uptick in the pursuit of novel technology that can aid in the fight against the COVID-19 pandemic, and this effort is ongoing [5,6]. To assist medical researchers, many machine learning professionals have offered their skills for free. Machine learning has the potential to be applied in various other areas, including the detection of COVID-19 patients from chest X-ray images. The presence or absence of infection can be determined by analyzing the X-ray chest image of the study participant using a deep learning-based algorithm. Numerous scientists are now investigating this question [7-9]. When employing ENN, the proposed model is presented in Figure 1.

The selection of the research object, in this case, COVID-19 detection using chest X-ray images, was driven by the urgent need for accurate and efficient diagnostic methods to combat the global COVID-19 pandemic [10,11]. Chest X-ray imaging is a widely available and relatively inexpensive tool that can support the clinical diagnosis of COVID-19, particularly in resource-limited settings. By developing a reliable and efficient method for COVID-19 detection from chest X-ray images, healthcare professionals can benefit from a faster and more accessible diagnostic approach. However, it is essential to acknowledge the limitations of applying the results obtained. First, the proposed method relies on the availability of high-quality chest X-ray images, which may not always be feasible in real-world scenarios where image quality can vary [12].

Additionally, the research utilized a specific dataset consisting of X-ray images from the Medical Centre of Bahawalpur and Kaggle, which may not fully represent the diversity of cases encountered in different regions or populations. Furthermore, while the proposed method achieved high accuracy rates on the tested dataset, it is essential to validate the approach on larger and more diverse datasets to ensure its generalizability [13,14,15].

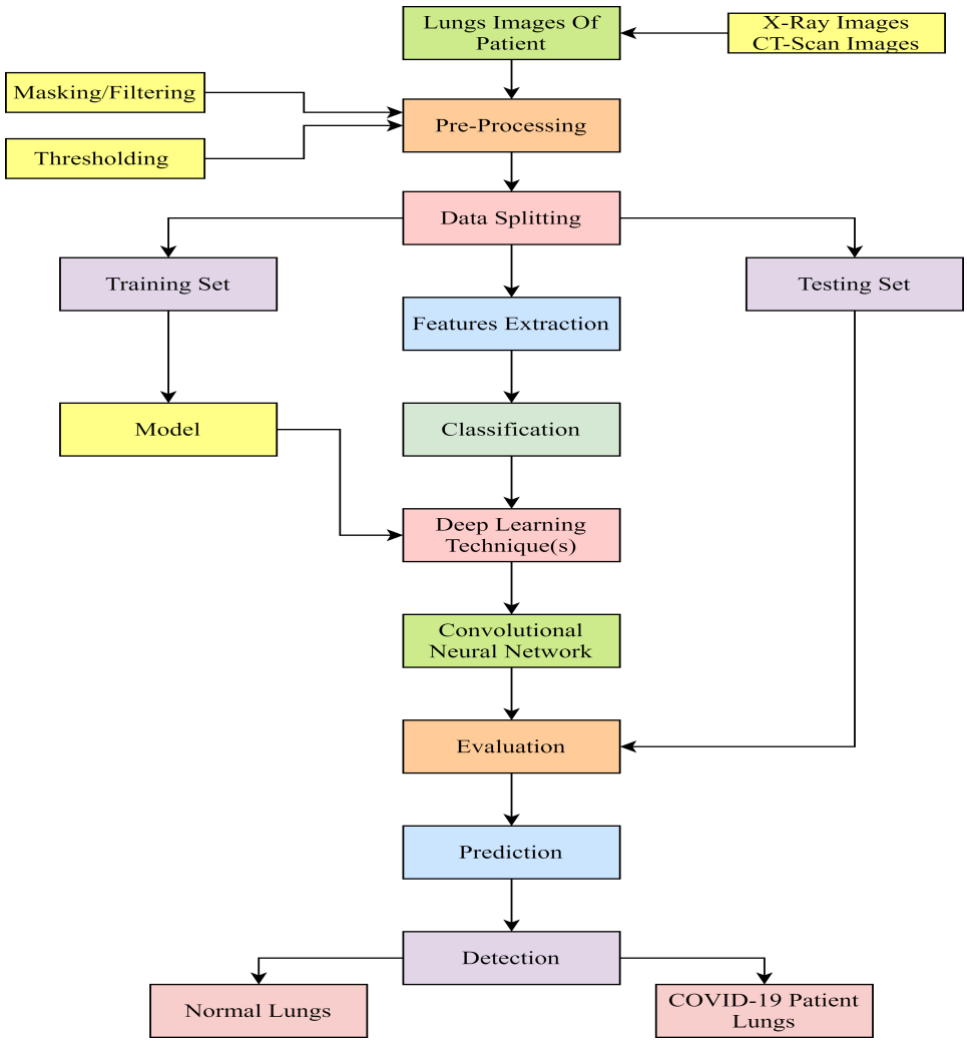

Figure 1: Proposed methodology

The performance of the method may vary when applied to different datasets with varying levels of complexity and variability [14,15]. Therefore, further studies and validation on larger datasets and in various clinical settings are necessary to assess the robustness and effectiveness of the proposed method. In summary, while the research objective of COVID-19 detection using chest X-ray images is selected to address an urgent need, the limitations regarding image quality, dataset representativeness, and the need for further validation must be acknowledged. Future research should focus on addressing these limitations to ensure the reliable and widespread application of the obtained results.

2.1. Dataset collection and description

This research utilized X-ray images collected from Kaggle sources. Patients with both standard and pathological conditions (COVID-19) are represented in the Images collection. The data collection includes four conditions: COVID-19, Pneumonia, Normal and lung opacity. The database serves as an index to volumes and cases. Images and information gathered during a single positive COVID-19 assessment constitute a "case." Volumes are just collections of cases bundled together for the convenience of distribution. Each case may have anything from six to ten associated documents. Here are a few examples of the information that was compiled as part of the dataset. Figure 2 shows Samples collected from the

COVID-19 Kaggle dataset. We will use a subset of the original dataset from which we trained the model for this particular application. The model may help doctors spot cases of COVID-19 more quickly. Using a trained dataset of X-ray scans, identify instances of COVID-19.

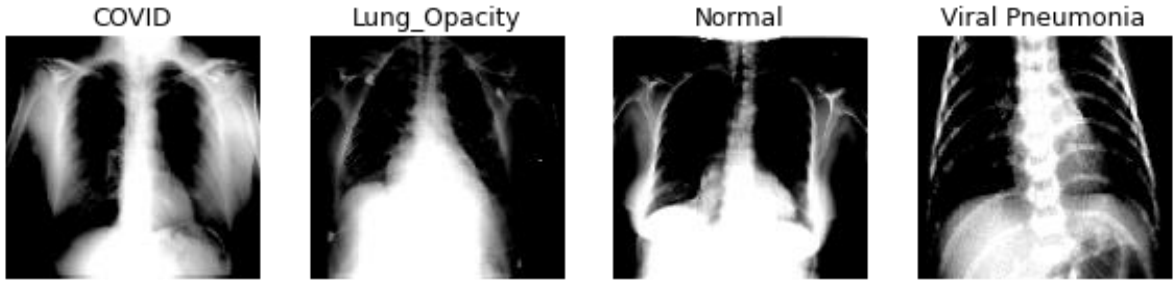

Figure 2: Samples collected from the COVID-19 Kaggle dataset

The test set consists of only 400 images, while the training set contains 10,000 chest X-rays. Classes in the collection provide either favorable or unfavorable examples of COVID-19. The dataset is split into training and testing sets to guarantee accurate results. Seventy percent of available data sets are used for model building, whereas only 30 percent are utilized in model evaluation. This section is also included in the same data collection.

2.2. Pre-processing techniques

The detection of COVID-19 is dependent on the frame fault. The author achieves a genuinely positive and false positive rating by calculating various error rates, which are used to pinpoint the area under the receiver operating characteristic curve (AUC). The Equal Error Rate (EER) occurs when the number of false positives and false negatives is equal. Figure 3 shows an X-ray image of Normal Lungs, while Figure 4 shows an X-ray image of a COVID-19 patient.

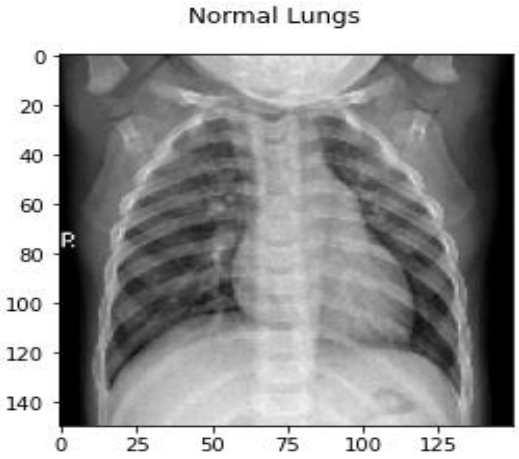

Figure 3: X-Ray image of normal lungs

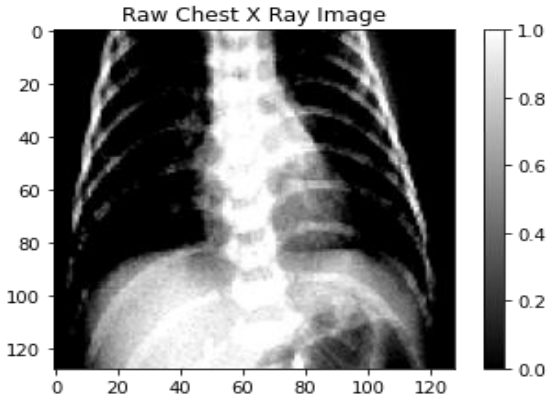

Figure 4: COVID-19 patient

2.3. Classification

During the session, several machine learning methods are examined and evaluated. The goal of any machine learning method is to produce a pattern or model that can be used for data classification from what is known as a training dataset (thus, this time, with corresponding responses from the classifier class) [16,17]. The accuracy of the model is checked against data from a separate source (the validation dataset). The fundamental algorithms used by the learning technology govern how the model is built. The most typical approach to this research is summarized here.

The use of data for "learning" can be accomplished in two broad ways [18,19]. Supervised learning and unsupervised learning are the terms used to describe these two types of training. To function appropriately, supervised learning techniques typically require "non-hidden" or "non-limited" input data in the form of feature vectors or other feature matrices. A function that accepts a wide variety of inputs and returns only the desired result is required [20,21]. Various machine learning algorithms aim to achieve this goal. The key difference between supervised and unsupervised learning is that in the latter, the learner is not shown the output vector. One of the primary functions of an unsupervised learning system is to categorize information into meaningful groups [22,23,24]. It takes its input from the data vector. With these categories, we can check whether the patterns of output meet expectations. Figure 5 shows the Classes of Datasets.

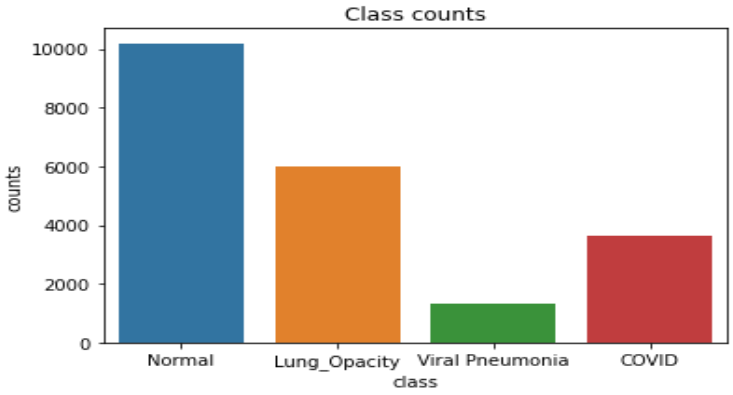

Figure 5: Classes of datasets

2.4. Efficient Neural Network (ENN)

ENN is very effective in classifying data and recognizing images. Enhanced naive neural networks (ENNs) are helpful for object and person recognition. In oncology, ENNs are most often employed for

detecting retinal phenotype. An ENN's input layer accepts standardized image data of the same size. After that, the images are processed by the efficient layer that is the foundation of ENN. This layer automatically learns a vast number of filters in parallel with a dataset, making it well-suited for tackling large-scale predictive problems, such as classification. The resulting characteristics are one-of-a-kind but also present elsewhere in the raw image. This stage includes 64 units and a 3x3x3 kernel. We then process our data by passing it via another core component of our ENN, the pooling layer. Its purpose is to gradually reduce the spatial dimension of the image, thereby reducing the computational requirements and network parameters. It can be used independently on any feature map. An effective pooling layer is the Max-pooling layer, which has a 2x2x2 kernel. Following this layer, we have a Fully Linked Layer, where all our data undergoes final processing. This layer receives promotion from neural networks. The output of the pooling layer is used as the input to the next fully connected layer. The pooling layer starts out being compressed and then serves as a fully connected layer. The output layer, or dense layer, takes the information from the previous layers and compresses and transforms it into the desired number of classes. Figure 6 shows the proposed ENN technique for classification. The entire ENN is shown in Figure 6.

The Efficient Neural Network (ENN) model architecture can be described mathematically using the following equations:

Input Layer: The input layer receives the chest X-ray image data as input. If the chest X-ray image has n pixels, then the input layer has n neurons. The output of the input layer is denoted as X, which is a vector of length n.

Hidden Layers: The ENN model has multiple hidden layers, each containing a set of neurons. The output of each hidden layer is computed using the following equation:

$$Z(l) = w(l) * A(l-1) + b(l)$$

Where Z(l) is the output of the first hidden layer, w(l) is the weight matrix of the first layer, A(l-1) is the activation vector of the previous layer, and b(l) is the bias vector of the first layer.

The activation function used in the hidden layers can be any non-linear function, such as ReLU or sigmoid. Let f(x) denote the activation function.

The output of the first hidden layer is denoted as A(l) and is computed as:

$$A(l) = f\big(Z(l)\big)$$

Output Layer: The output layer of the ENN model consists of a single neuron, representing the binary classification output (COVID-19 positive or negative). The output of the output layer is computed using the following equation:

$$Y = w(L+1) * A(L) + b(L+1)$$

Where Y is the output of the output layer, w(L+1) is the weight matrix of the output layer, A(L) is the activation vector of the last hidden layer, and b(L+1) is the bias vector of the output layer.

The activation function used in the output layer can be the sigmoid function, which ensures that the output value is between 0 and 1.

Optimization: To optimize the ENN model, various optimization algorithms can be employed. The three optimization algorithms mentioned in the paragraph are ADAM, SGD, and RMSProp. Each optimization algorithm updates the weight and bias parameters of the ENN model using a different approach.

ADAM optimizer: The ADAM optimizer combines the advantages of two other optimization algorithms, namely RMSProp and Momentum. It maintains two moving averages of the gradients and the

gradient squares, and uses them to update the parameters. The weight and bias updates using ADAM can be expressed as:

$$m(t) = beta1 * m(t-1) + (1 - beta1) * dw$$

$$v(t) = beta2 * v(t-1) + (1 - beta2) * (dw^2)$$

$$w(t) = w(t-1) - alpha * \left(\frac{m(t)}{(sqrt(v(t)) + epsilon)}\right)$$

$$b(t) = b(t-1) - alpha * \left(\frac{mb(t)}{(sqrt(vb(t)) + epsilon)}\right)$$

SGD optimizer: The SGD optimizer updates the weight and bias parameters using the gradient of the loss function for the parameters. The weight and bias updates using SGD can be expressed as:

$$w(t) = w(t-1) - alpha * dw\, b(t) = b(t-1) - alpha * db$$

Where dw and db are the gradients for the weights and biases, and alpha is the learning rate. The RMSProp algorithm computes a moving average of the squared gradients and divides the gradient by the root of this average. This enables the algorithm to adjust the learning rate of each weight parameter according to the magnitude of its gradient. This helps prevent the learning rate from becoming too large or too small, which can cause slow convergence or oscillations.

The RMSProp update rule for a weight parameter w at time step t with learning rate alpha, decay rate rho, and small constant epsilon is:

g_t = gradient of loss function for w at time step t

$$s_t = rho * s_{\{t-1\}} + (1 - rho) * g_t^2$$

$$w_t = w_{\{t-1\}} - alpha * \frac{g_t}{(sqrt(s_t) + epsilon)}$$

Here, g_t is the gradient at time step t, s_t is the moving average of the squared gradients up to time step t, rho is the decay rate (usually set to 0.9), alpha is the learning rate, and epsilon is a small constant to prevent division by zero.

In this way, RMSProp adapts the learning rate of each weight parameter based on the magnitude of its gradients, allowing for faster and more accurate convergence.

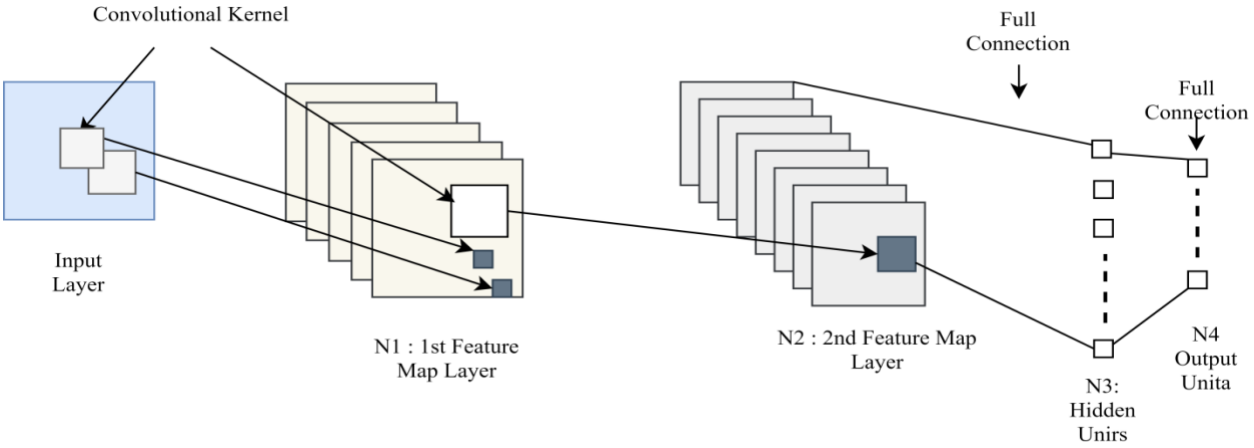

Figure 6: Proposed ENN technique for classification

2.5. Optimized ENN model

The ultimate purpose of machine learning is to narrow the gap between actual and expected results [25,26]. It is common to refer to the cost function as a "loss function" (C). One quality of costs is their convexity. Finding the optimal weight value will enable the most significant possible improvement in the cost function [27,28]. Additionally, we need to ensure that the method could be applied in various other contexts. Thus, it is easier to make accurate predictions on as-yet-unobserved data. Accordingly, Figure 7 shows the Optimized ENN Model Working.

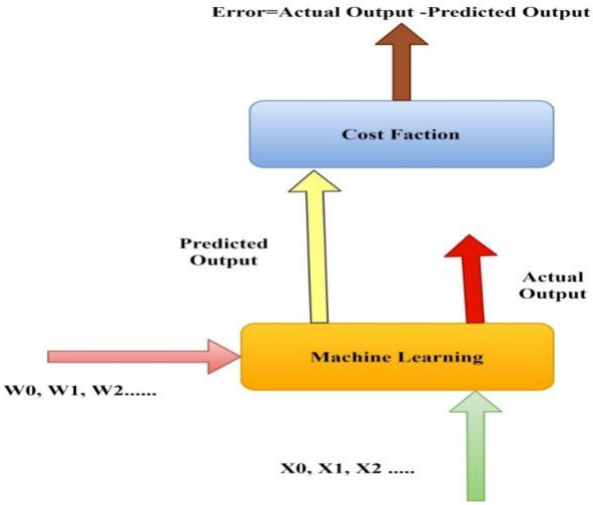

Figure 7: Optimized ENN model working

2.6. Gradient-based learning

We perform multiple iterations with varying weights. In turn, this facilitates determining the lowest possible price. An example of a gradient descent is shown below.

2.6.1. Gradient descent

Gradient descent is a machine learning technique used to incrementally decrease a cost function. The precision of models benefits from this. The gradient represents the increase. We need to reverse course and look for the valley's bottom. To minimize damage, it is best to implement negative adjustments to the parameters.

$$\theta = \theta - \eta \nabla J(\theta; x, y)$$

The weight parameter, the learning rate, and the weight parameter gradient are J(x,y). θ

2.6.2. Gradient descent types

There are several ways to quantify the derivative function of the cost for the gradient descent. The time complexity and precision of an algorithm are both impacted by the amount of data it processes. Here are some examples of each type:

- Mini batch
- Batch Gradient Descent
- Stochastic Gradient Descent

2.6.3. Role of an optimizer

Optimizers adjust the weight parameters to minimize losses. Whether or not the optimizer is making progress toward the global minimum in the valley ground is indicated by the loss function.

2.6.4. Types of optimizers

2.6.4.1 Momentum

Momentum is like a ball rolling downhill. As it rolls down the hill, the ball gains Momentum.

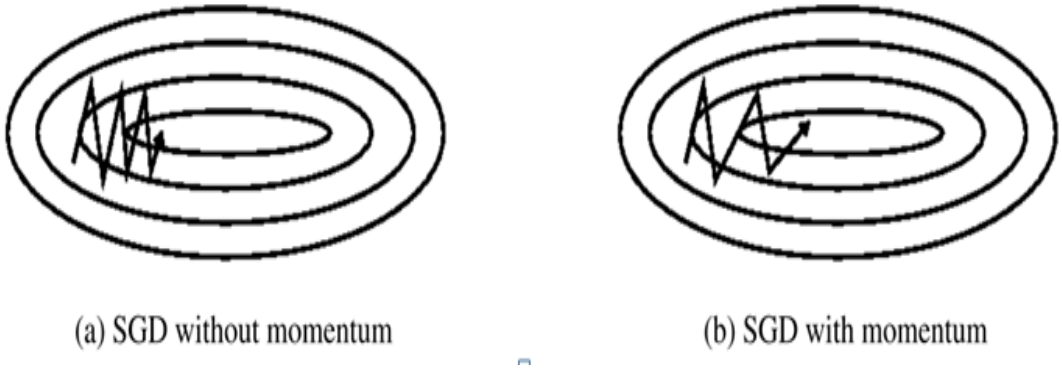

Figure 8: SGD model relation with momentum

Figure 8 illustrates the relationship between the SGD Model and Momentum. When the surface curves more steeply in one direction than another, Momentum aids in the rapid descent of the gradient. As can be seen up top, the swing also serves to dampen.

$$v_t = \gamma v_{t-1} + \eta \nabla J(\theta; x, y)$$
$$\theta = \theta - v_t$$

The Gradient descent takes into account the gradient of previous steps.

2.6.4.2 Nesterov accelerated gradient (NAG)

Nesterov's acceleration optimization is similar to rolling a ball down a hill, but he knows when to let off the gas before the ball reaches the top. For both this iteration and the next, the gradient needs to be calculated. Change the weights of factors to reflect how much weight you give to each element. Figure 9 shows NSG Nesterov momentum.

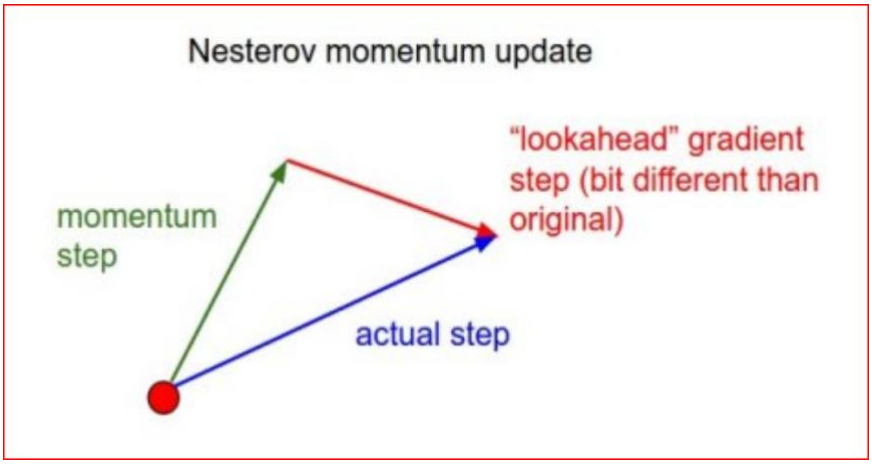

Figure 9: NSG Nesterov momentum

.

$$\theta = \theta - v_t$$
$$v_t = \gamma v_{t-1} + \eta \nabla J(\theta - \gamma v_{t-1})$$
$\theta - \gamma v_{t-1}$ is the gradient of looked ahead

2.6.4.3 RMSProp

To describe this method, we use the abbreviation "Root Mean Square Propagation" (RMSProp). Geoffrey Hinton is solely responsible for the conception and development of the idea. RMSProp attempts to address the drastically reduced learning rates observed with Adagrad by employing a method called a moving average squared gradient.

The RMSProp study rate will be automatically updated, and the research rate for each parameter will be chosen independently of the overall rate. Root Mean Square Propagation (RMSProp) employs the exponential decay of the gradients as a dividing factor to get the average learning rate between squared gradients.

$$\theta_{t+1} = \theta_t - \frac{\eta}{\sqrt{(1-\gamma)g^2{}_{t-1} + \gamma g_t + \varepsilon}} \cdot g_t$$

β is the decay term, which takes a value from 0 to 1. gt moves an average gradient of squared

2.6.4.4 Adam — Adaptive Moment Estimation

Adam is another technique that uses the first and second instant estimates to determine the adaptive learning rate for each parameter [29,30]. Learning rates in Adagrad, which are already low, are further reduced. Adam is a combination of the online and non-stationary RMSProp and sparse gradient methods known as Adagrad [31].

The Adam method revises the average of the squared gradient and the average of the exponentially moving momenta of the first and second moments (vt). As illustrated below, the hyperparameters 1, 2, and 1 [0, 1] determine the exponential decay rates of these motions.

$$m_t = \beta_1 m_{t-1} + (1-\beta_1) g_t$$
$$v_t = \beta_2 v_{t-1} + (1-\beta_2) g_t^2$$

m_t and v_t are estimates of first and second moment respectively

In the earliest steps, in particular, instantaneous estimates of zero occur because moving averages are initialized as zero. It is simple to eliminate this start-up division and obtain skewed estimates.

$$\hat{m}_t = \frac{m_t}{1-\beta_1^t}$$
$$\hat{v}_t = \frac{V_t}{1-\beta_2^t}$$

$\hat{m}_t$ and $\hat{v}_t$ are bias corrected estimates of first and second moment respectively

Finally, as shown below, we update the parameter.

$$\theta_{t+1} = \theta_t - \frac{\eta \hat{m}_t}{\sqrt{\hat{v}_t + \varepsilon}}$$

2.7. Performance Parameters

Accuracy, sensitivity, specificity, and area under the curve (AUC) are all used to verify the validity of the proposed method. All of these ongoing efforts are tied to the optical and parametric results of the new method. The formulas below are used to derive the suggested method's performance metrics:

2.7.1. Accuracy

The quality or condition of being correct, honest, or precise is referred to as accuracy.

$$\text{Accuracy} = (\text{TP} + \text{TN})/(\text{TP} + \text{TN} + \text{FP} + \text{FN})$$

2.7.2. Area under the Curve

The AUC is calculated by integrating the signal between two locations at a constant rate. Suppose you know that y = f(x) between x = a and b, then you can calculate the AUC by integrating y = f(x) between the limits of a and b. This is accomplished by jointly specifying and integrating the constraints of types A and B. The mathematical representation of accuracy is

$$\text{AUC} = (\text{Sensitivity} + \text{Specificity})/2$$

2.7.3. Sensitivity

When discussing diagnostic tests, sensitivity refers to a test's ability to accurately identify patients who are sick or unhealthy. Accuracy is expressed mathematically and presented in Section 3.3

$$\text{Sensitivity} = \text{TP}/(\text{P} + \text{FN})$$

3. Results and Discussion

3.1. RMSProp Optimization

We consider the optimizer RMSProp and illustrate how well the model performs on the COVID-19 training and testing sets. With a minimum validation loss of 0.26, the model achieves an accuracy of 88.93% on the training set and 95% on the test set for correctly categorizing data. The following images display the outcomes of an ENN that has been optimized using RMSProp: Figure 10 shows RMSProp optimization

model accuracy. Figure 11 shows the RMSProp Optimization model loss, while Figure 12 shows classification using RMSProp.

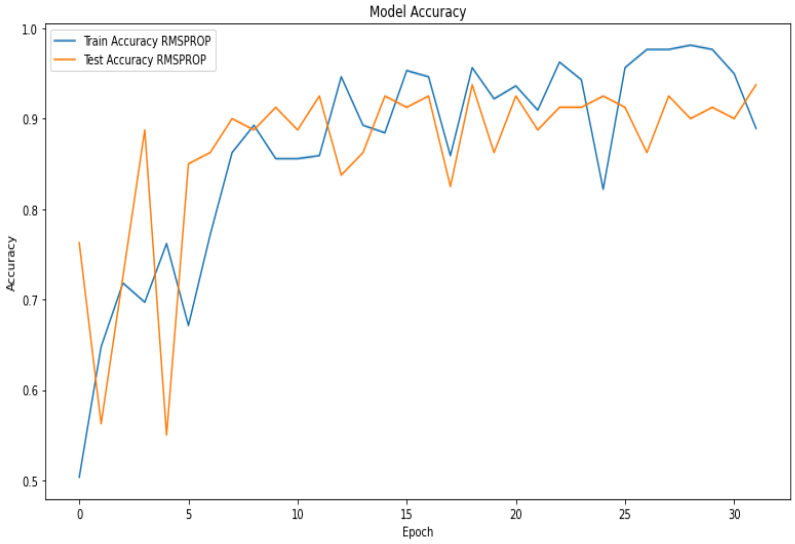

Figure 10: RMSProp optimization model accuracy

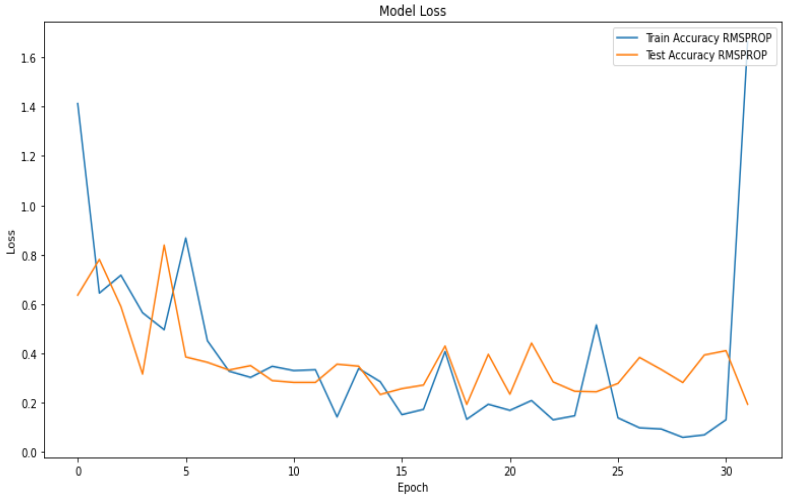

Figure 11: RMSProp optimization model loss

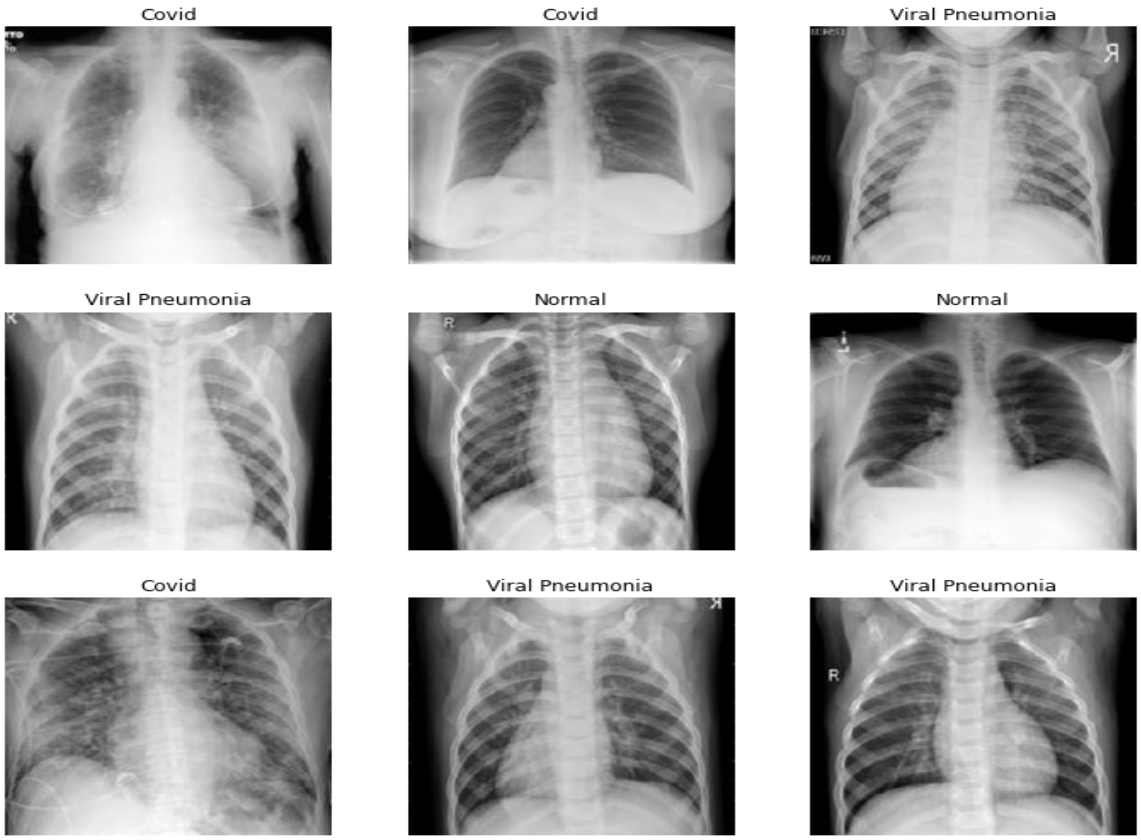

Figure 12: Classification using RMSProp

3.2. SGD Optimization

In the following figures, we consider an SGD optimizer and illustrate the performance of the COVID-19 model on both the training and testing sets. With a minimum validation loss of 0.25, the model achieves an accuracy of 92.62% on the training set at epoch 32. In contrast, the testing accuracy, which measures the correct classification of the proper class at the same epoch, approaches 95%. The figures below display the results of an ENN that has been optimized using SGD: Figure 13 shows SGD optimization accuracy. Figure 14 shows the SGD optimization loss, while Figure 15 shows classification using SGD.

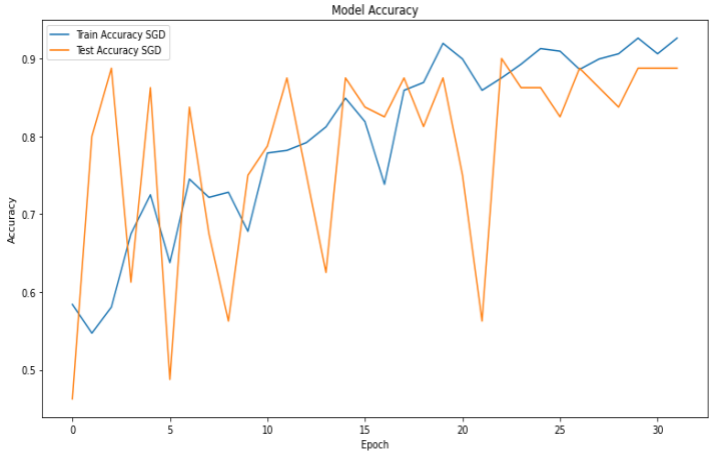

Figure 13: SGD optimization accuracy

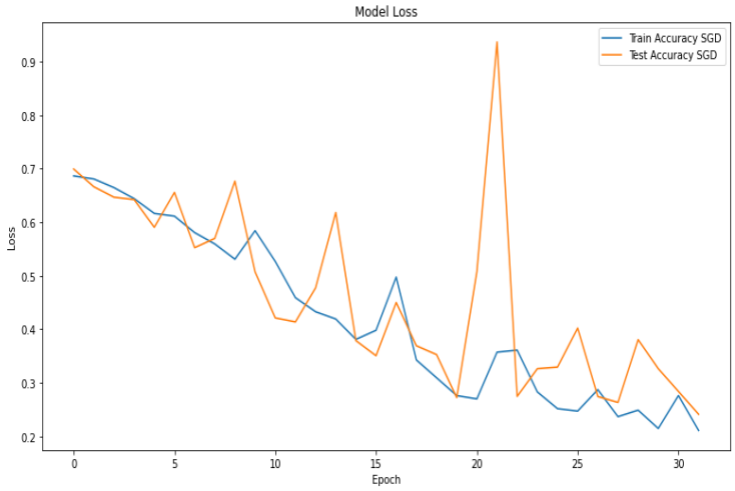

Figure 14: SGD optimization loss

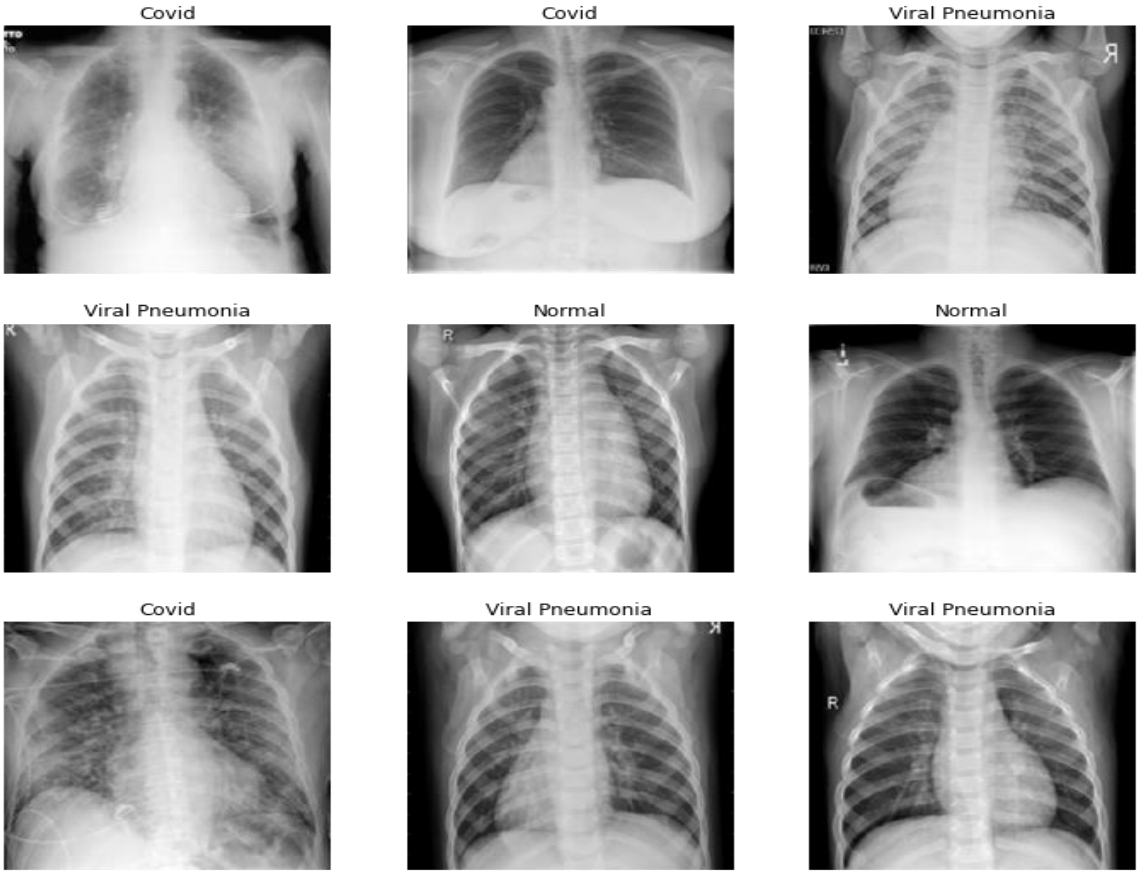

Figure 15: Classification using SGD

3.3. ADAM optimization

Work on the ADAM optimizer using ENN has been completed. See below for graphical depictions of COVID-19 model correctness on both the training and testing sets, with ADAM as the optimizer of interest. With a validation loss of 0.18, the model achieves 98.99% accuracy on the training set at epoch 32, whereas the accuracy of the test set approaches 95.00% at the same epoch. The following images illustrate the

enhanced ENN performance achieved by using ADAM: Figure 16 shows the ADAM optimization model accuracy. Figure 17 shows the ADAM optimization model loss. While Figure 18 illustrates classification using ADAM, Figure 19 displays the confusion matrix for classification.

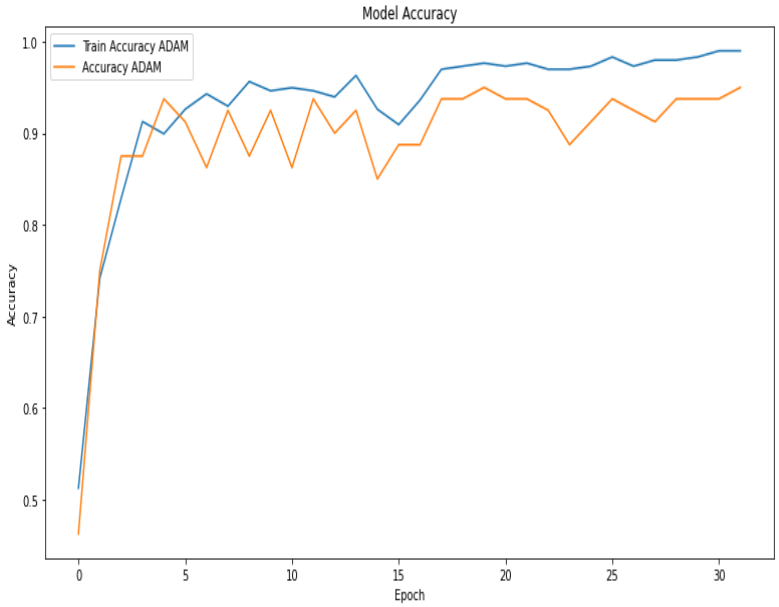

Figure 16: ADAM optimization model accuracy

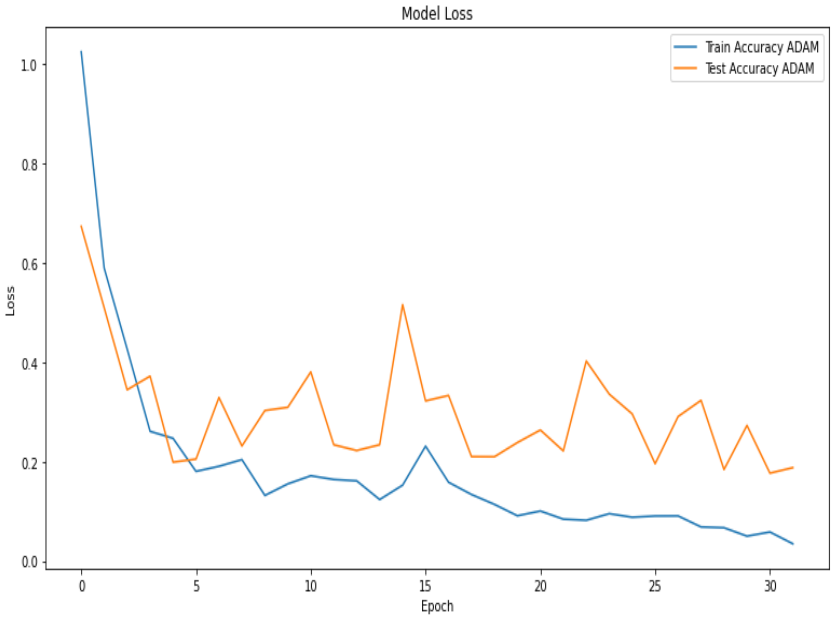

Figure 17: ADAM optimization model loss

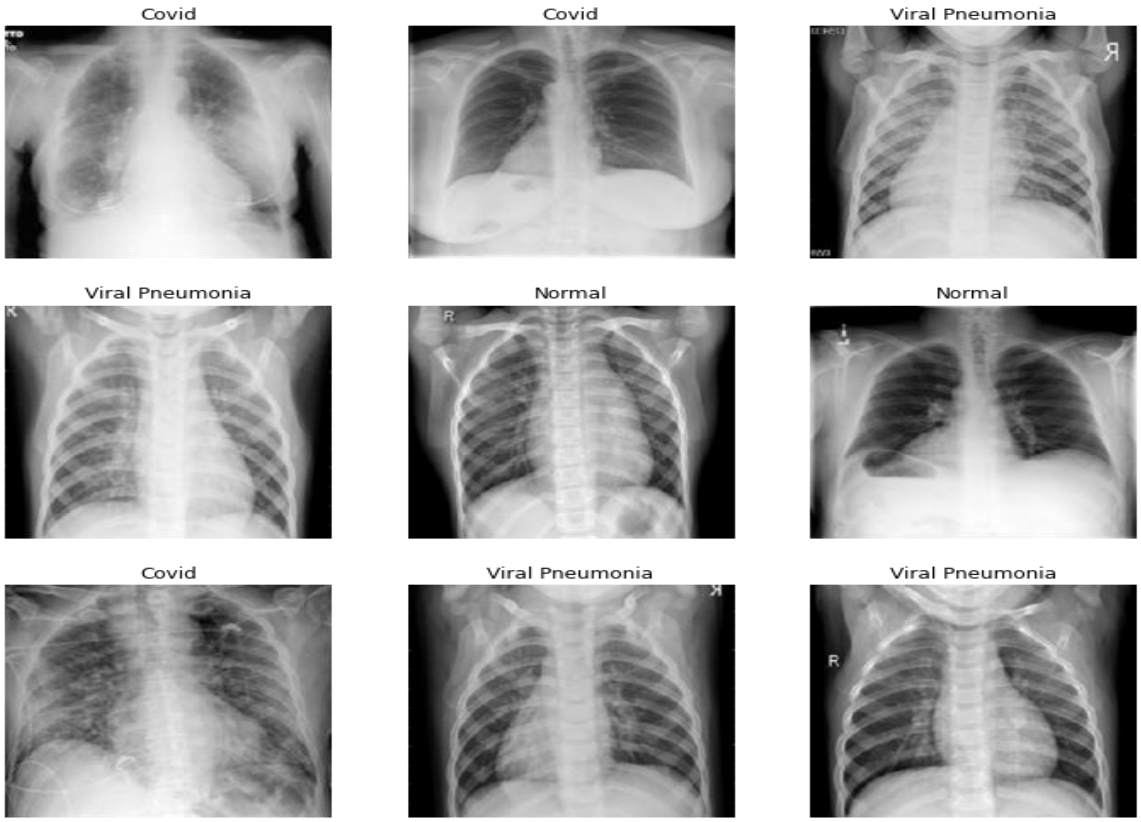

Figure 18: Classification using ADAM

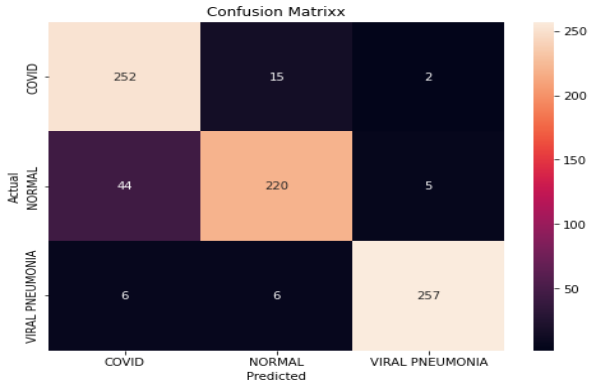

Figure 19: Confusion matrix for classification

3.4. Discussion of results

ENN excels as a binary classifier on the chest X-ray dataset. However, when optimizations were substituted for non-optimized methods, classification accuracy increased dramatically. ADAM's success rate of 95% was the highest of the three. Among the three optimization strategies, only ADAM (98.99%) achieved training accuracy above 95%; RMSProp (88.8%) and SGD (89.0%) fell short (92.62%). Despite having to work with images that were reduced in size by more than half their original size, the algorithm in this research was nevertheless able to identify COVID-19 cases correctly.

We presented an approach that provides a robust answer to the problem of eliminating noise during processing. The chest X-ray images were used, despite being speckle-attacked and of poor quality. The test

images were pre-processed to remove speckle noise. This strategy is effective at eliminating background noise. In this way, the input images could be pre-processed to improve feature extraction and, in turn, classification precision. Our findings suggest that the proposed optimization strategy can facilitate the speedy and accurate diagnosis of COVID-19, which in turn can help clinicians take the necessary steps to preserve the lives of patients infected with the virus.

4. Comparisons in state of the art

In comparison with existing methods, as shown in the Table 1, the proposed method in this research achieved a high accuracy rate of 98.99% when using X-ray images from the Kaggle dataset for COVID-19 detection. Let us examine the performance of the proposed method based on the results reported in previous studies: This research reported an accuracy rate of 93.1% when using real chest X-ray (CXR) images for COVID-19 detection [1]. It is worth noting that authentic CXR images may present additional complexities compared to curated datasets, such as Kaggle, which could impact performance. In this research, an accuracy rate of 96.13% was achieved using X-ray images from the Kaggle dataset [2]. The proposed method in the present research outperforms this method with a higher accuracy of 98.99% [3]. In this research an accuracy rate of 97.97% was reported when utilizing X-ray images from the Kaggle dataset. The proposed method surpasses this result by achieving an accuracy rate of 98.99%. In this research, an accuracy rate of 98.53% was attained using X-ray images from the Kaggle dataset. Although the proposed method in the present research achieves a slightly higher accuracy of 98.99%, the difference between the two methods is relatively small [4].

Overall, the proposed method in this study demonstrates competitive performance in COVID-19 detection using chest X-ray images when compared to existing methods. It outperforms some previous studies and achieves a comparable accuracy rate to others. However, it is essential to consider factors such as dataset variations, methodology, and the specific characteristics of the patient population when interpreting and comparing the results. The results of the present study on COVID-19 detection using chest X-ray images and efficient neural network techniques demonstrate the effectiveness of the proposed approach. The study employed an efficient neural network architecture trained with multiple optimizers, including RMSProp, SGD, and ADAM, to automatically extract relevant features from chest X-ray images and accurately classify COVID-19 cases. The performance of the proposed models was evaluated using various metrics, including accuracy, sensitivity, specificity, and area under the curve (AUC). The models were trained and tested on a dataset consisting of the COVID-19 Kaggle dataset. The training set comprised 10,000 chest X-rays, while the test set contained 400 images. Comparing the optimization models, the results indicate that the model using the ADAM optimizer outperformed the other models. It achieved a validation loss of 0.18 and attained 98.99% accuracy on the training set at epoch 32. Moreover, with 32 epochs, the model's accuracy on the test set reached 95.00%.

These results highlight the superiority of the ADAM optimizer in correctly classifying X-ray images of COVID-19 patients. To further analyze the performance of the proposed method, a comparison with previous studies is warranted. Table 1 provides a comparison of the proposed method with four existing studies on COVID-19 detection using chest X-ray images. The proposed method achieved an accuracy rate of 98.99% on the Kaggle dataset, surpassing the accuracy rates reported in the previous studies, which ranged from 93.1% to 98.53%. This indicates the competitive performance of the proposed method in accurately detecting COVID-19 cases. It is essential to consider the limitations of the proposed method when interpreting its performance. One limitation is the reliance on curated datasets, such as the Kaggle dataset, which may not fully represent the complexity and variability of real-world cases.

Additionally, the research acknowledges the potential variations in image quality and the need for further validation on larger and diverse datasets to ensure the generalizability of the results. The high accuracy and effectiveness demonstrated by the proposed method hold promise for its application as a valuable tool in efficiently triaging and managing COVID-19 patients. However, future research should focus on addressing the limitations and conducting more extensive validation studies to assess the method's performance in real-world clinical settings. In conclusion, this study presents a comprehensive analysis of the results obtained in COVID-19 detection using chest X-ray images. The proposed method outperforms previous studies in terms of accuracy, demonstrating the effectiveness of efficient neural network techniques. While the results are promising, further research is needed to overcome the limitations and ensure the reliable application of the proposed method in real-world scenarios.

Table 1: Comparison with existing methods

Reference	Method	Data	Type	Accuracy
de Moura et al. [31]	Fully automatic deep convolutional approaches	Chest X-Ray	COVID-19, Pneumonia, Normal	96.5%
Verma et al. [32]	Deep learning with histogram equalization and lung segmentation	Chest X-Ray	COVID-19, Pneumonia, Normal	95.8%
Chakraborty & Mali [33]	Super pixel-based fuzzy image segmentation (SUFEMO)	Chest CT	COVID-19, Pneumonia, Normal	94.7%
Gtifa et al. [34]	Animal Migration Optimization, Electro-magnetism-like Optimization, Harmony Search Algorithm	Chest X-Ray	COVID-19, Pneumonia, Normal	99.00%
Anakal & Uppin [35]	ResNet-34- based deep learning mode	Chest X-Ray	COVID-19, Pneumonia, Normal	98%
Li et al. [36]	COVNet (Based on ResNet50)	Chest CT	COVID-19, Pneumonia, Normal	96%
Tuncer et al. [37]	A Novel Exemplar Chest Image Classification Method	Chest X-Ray	COVID-19, Pneumonia, Normal	97.01%
Wajeeha et al.	Proposed Method	Chest X-Ray	COVID-19, Pneumonia, Normal	**98.99%**

5. Conclusion

The major acute respiratory syndrome coronavirus-2 that produced the horrific COVID-19 epidemic has wreaked havoc on healthcare systems throughout the world (SARS-CoV-2). Several issues and difficulties are currently associated with testing for the illness, which is why new, more effective approaches that are also cost-effective must be developed. Identifying the presence of COVID-19 in chest X-ray images is one area where machine learning (ML) has emerged as a powerful predictive approach in recent years. This article presents the results of an experiment demonstrating the effectiveness of using a Deep Learning Method (DLM) to identify COVID-19 in chest X-ray pictures (CXR). In comparison to more involved and costly pathological testing, radiographic images are easily obtained and can be used efficiently for COVID-19 detection. Among the 10,040 samples tested, 2,143 were positive for COVID-19, 3,674 were positive for pneumonia (but not for COVID-19), and 4,223 were negative for both diseases (neither COVID-19 nor pneumonia). Our model performed admirably, achieving a detection accuracy of 96.43% and a sensitivity of 93.68%. Normal patients had an AUC of 98.99%, while those with pneumonia (which tested negative for COVID-19) had an AUC of 97%.

The proposed research contributes to the field of medical imaging by presenting an efficient method for detecting COVID-19 from chest X-ray images. By leveraging advanced neural network techniques and transfer learning, the proposed models demonstrate high accuracy in identifying COVID-19 cases. This contributes to the ongoing efforts in developing practical diagnostic tools for COVID-19. By combining these diverse datasets, the study enhances the robustness and generalization capabilities of the models. This contributes to the advancement of COVID-19 detection research by incorporating real-world data from different sources. The study evaluates the performance of the proposed models using various evaluation metrics and compares them with other existing approaches. This comparative analysis showcases the effectiveness of the proposed method and highlights its potential to outperform traditional diagnostic methods. These contributions collectively advance the field of medical imaging and contribute to the development of reliable diagnostic tools for COVID-19.

5.1. Prospective research

This research article proposed an Efficient Neural Network (ENN) model optimized using three algorithms (ADAM, RMSProp, and SGD) for COVID-19 detection using chest X-ray images. The model leveraged transfer learning utilizing feature extraction from pre-trained CNNs, classification performed by a support vector machine SVM model, and image pre-processing (including noise removal and resizing). Optimization achieved using SGD, RMSProp, and ADAM. ADAM outperformed the other optimizers, achieving 98.99% training accuracy and 95% test accuracy. The research comprised two datasets from Kaggle and the Bahawalpur hospital. Included four classes: COVID-19, Pneumonia, Normal, and Lung Opacity, with 10,000 images for training and 400 for testing.

This research contributed to the introduction of ENN, along with optimization strategies, for the detection of COVID-19. The study achieved a performance benchmark against other studies and demonstrated competitive accuracy. A performance comparison was conducted among three optimizers using the same architecture. While transfer learning and CNNs are widely used, combining ENN with optimizer benchmarking and local data adds modest novelty. ADAM optimization insights for future research dimensions. Although the research utilized real and publicly available data sources, performance evaluation conducted with multiple optimizers and accuracy were achieved through well-organized sections; however, there is still room for improvement. Future research could validate the external datasets, increase the test size, and expand the role of transfer learning models. Future work may include the incorporation of additional datasets from other hospitals or sources to enhance generalizability and reduce biases with Kaggle and small local datasets. Cross-validation, including k-fold, may generate more reliable performance metrics. ROC and Confusion Matrix Plots can be analyzed in more depth.

Funding: No specific funding received for this research.

Data Availability: The data that support the findings of this study are available from the corresponding author upon reasonable request.

Conflicts of Interest: No conflict of interest is stated by the author.

Authors contributions. Conceptualization: WM, RJ, MAR; methodology: WM, RJ, FT, MAR; software: WM, RJ; validation: FT, MAR; writing—original draft preparation, WM, RJ, FT; writing—review and editing: WM, MAR, visualization: FT, MAR; supervision: FT, MAR; project administration: RJ, FT, MAR; all authors had approved the final version.

References

[1] Prince, R., Niu, Z., Khan, Z. Y. et al., (2025). "Interpretable COVID-19 chest X-ray detection based on handcrafted feature analysis and sequential neural network", *Computers in Biology and Medicine*, 186, 109659.

[2] El Asnaoui, K., and Chawki, Y. (2021). "Using X-ray images and deep learning for automated detection of coronavirus disease", *Journal of Biomolecular Structure and Dynamics*, 39(10), 3615-3626.

[3] Elhajjej, M. H., Said, S., Arfaoui, N. et al., (2025). "Asynchronous and Flexible Federated Learning for COVID-19 Detection from Chest X-Ray Images", *Journal of Advanced Computational Intelligence and Intelligent Informatics*, 29(4), 857-867.

[4] Sharma, S. (2020). "Drawing insights from COVID-19-infected patients using CT scan images and machine learning techniques: a study on 200 patients", *Environmental Science and Pollution Research*, 27(29), 37155-37163.

[5] Prabhu, V. S., and Thyagharajan, K. K. (2025). "Enhancing COVID-19 detection through multimodal CT and X-ray image fusion with anisotropic diffusion and loss-attentional physics-informed neural networks", *Biomedical Signal Processing and Control*, 110, 108200.

[6] Harmon, S. A., Sanford, T. H., Xu, S. et al., (2020). "Artificial intelligence for the detection of COVID-19 pneumonia on chest CT using multinational datasets", *Nature communications*, 11(1), 4080.

[7] AM, A.R., Giri, J., Ahmad, N. and Badawy, A.S. (2024). "Detection of Covid-19 based on convolutional neural networks using pre-processed chest X-ray images", *AIP Advances*, 14(3).

[8] Rahimzadeh, M., Attar, A., and Sakhaei, S. M. (2021). "A fully automated deep learning-based network for detecting COVID-19 from a new and large lung CT scan dataset", *Biomedical Signal Processing and Control*, *68*, 102588.

[9] Hammoudi, K., Benhabiles, H., Melkemi, M. et al., (2021). "Deep learning on chest X-ray images to detect and evaluate pneumonia cases at the era of COVID-19", *Journal of medical systems*, 45(7), 75.

[10] Khattab, R., Abdelmaksoud, I. R., and Abdelrazek, S. (2024). "Automated detection of COVID-19 and pneumonia diseases using data mining and transfer learning algorithms with focal loss from chest X-ray images", *Applied Soft Computing*, 162, 111806.

[11] Rubin, G. D., Ryerson, C. J., Haramati, L. B. et al., (2020). "The role of chest imaging in patient management during the COVID-19 pandemic: a multinational consensus statement from the Fleischner Society", *Radiology*, 296(1), 172-180.

[12] Khanday, A. M. U. D., Rabani, S. T., Khan, Q. R. et al., (2020). "Machine learning based approaches for detecting COVID-19 using clinical text data", *International Journal of Information Technology*, 12(3), 731-739.

[13] Pascarella, G., Strumia, A., Piliego, C. et al., (2020). "COVID-19 diagnosis and management: a comprehensive review", *Journal of internal medicine*, 288(2), 192-206.

[14] Idilman, I. S., Telli Dizman, G., Ardali Duzgun, S. et al., (2021). "Lung and kidney perfusion deficits diagnosed by dual-energy computed tomography in patients with COVID-19-related systemic microangiopathy", *European radiology*, 31(2), 1090-1099.

[15] Rabbouch, B., Dkhil, M. B., Rabbouch, H. et al., (2025). "Refined Deep Learning Approaches for Enhanced COVID-19 Detection in Chest X-Ray Images", *Advances in Data Science & Adaptive Analysis*, 17.

[16] Sarkodie, B.D., Osei-Poku, K. and Brakohiapa, E., (2020). "Diagnosing COVID-19 from chest X-ray in resource limited environment-case report", *Med Case Rep*, 6(2), 135.

[17] Purohit, K., Kesarwani, A., Ranjan Kisku, D. et al., (2022, March). "Covid-19 detection on chest x-ray and ct scan images using multi-image augmented deep learning model", In *Proceedings of the Seventh International Conference on Mathematics and Computing: ICMC 2021* (pp. 395-413). Singapore: Springer Singapore.

[18] Sriwiboon, N. (2025). "Efficient and lightweight CNN model for COVID-19 diagnosis from CT and X-ray images using customized pruning and quantization techniques", *Neural Computing and Applications*, 37(18), 13059-13078.

[19] Das, A. K., Ghosh, S., Thunder, S. et al., (2021). "Automatic COVID-19 detection from X-ray images using ensemble learning with convolutional neural network", *Pattern Analysis and Applications*, 24(3), 1111-1124.

[20] El Houby, E. M. (2024). "COVID-19 detection from chest X-ray images using transfer learning", *Scientific Reports*, 14(1), 11639.

[21] Ahuja, S., Panigrahi, B. K., Dey, N. et al., (2021). "Deep transfer learning-based automated detection of COVID-19 from lung CT scan slices", *Applied Intelligence*, 51(1), 571-585.

[22] Singh, T., Mishra, S., Kalra, R. et al., (2024). "COVID-19 severity detection using chest X-ray segmentation and deep learning", *Scientific Reports*, 14(1), 19846.

[23] Asif, S., Qurrat-ul-Ain, Awais, M. et al., (2024). "A deep ensemble learning framework for COVID-19 detection in chest X-ray images", *Network Modeling Analysis in Health Informatics and Bioinformatics*, 13(1), 30.

[24] Dai, W., Zhang, H., Yu, J. et al., (2020). "CT imaging and differential diagnosis of COVID-19", *Canadian Association of Radiologists Journal*, 71(2), 195-200.

[25] Koyyada, S. P., and Singh, T. P. (2024). "A systematic survey of automatic detection of lung diseases from chest x-ray images: Covid-19, pneumonia, and tuberculosis", *SN Computer Science*, 5(2), 229.

[26] Che Azemin, M. Z., Hassan, R., Mohd Tamrin, M. I. et al., (2020). "COVID-19 deep learning prediction model using publicly available radiologist-adjudicated chest x-ray images as training data: preliminary findings", *International Journal of Biomedical Imaging*, 2020(1), 8828855.

[27] Buonsenso, D., Piano, A., Raffaelli, F., et al., (2020). "Novel coronavirus disease-19 pnemoniae: a case report and potential applications during COVID-19 outbreak", *Eur Rev Med Pharmacol Sci*, 24(5), 2776-80.

[28] Mohan, G., Subashini, M. M., Balan, S. et al., (2024). "A multiclass deep learning algorithm for healthy lung, Covid-19 and pneumonia disease detection from chest X-ray images", *Discover Artificial Intelligence*, 4(1), 20.

[29] Prince, R., Niu, Z., Khan, Z. Y. et al., (2025). "Interpretable COVID-19 chest X-ray detection based on handcrafted feature analysis and sequential neural network", *Computers in Biology and Medicine*, 186, 109659.

[30] Pradeep Dalvi, P., Reddy Edla, D., Purushothama, B. et al., (2024). "COVID-19 detection from Chest X-ray images using a novel lightweight hybrid CNN architecture", *Multimedia Tools and Applications*, 1-23.

[31] de Moura, J., Novo, J., and Ortega, M. (2022). "Fully automatic deep convolutional approaches for the analysis of COVID-19 using chest X-ray images", *Applied Soft Computing*, 115, 108190.

[32] Verma, K., Sikka, G., Swaraj, A. et al., (2024). "Classification of COVID-19 on chest X-Ray images using deep learning model with histogram equalization and lung segmentation", *SN Computer Science*, 5(4), 379.

[33] Chakraborty, S., and Mali, K. (2022). SUFEMO: "A superpixel based fuzzy image segmentation method for COVID-19 radiological image elucidation". *Applied Soft Computing*, 129, 109625.

[34] Gtifa, W., Mhaouch, A., Alsharif, N. et al., (2025). "Nature-inspired multi-level thresholding integrated with CNN for accurate COVID-19 and lung disease classification in chest x-ray images". *Diagnostics*, 15(12), 1500.

[35] Anakal, S., and Uppin, C. (2025). "Diagnosis of COVID-19 and viral pneumonia with chest x-ray images using ResNet-34", *Iraqi Journal for Computer Science and Mathematics*, 6(3), 6.

[36] Li, L., Qin, L., Xu, Z. et al., (2020). "Using artificial intelligence to detect COVID-19 and community-acquired pneumonia based on pulmonary CT: evaluation of the diagnostic accuracy", *Radiology*, 296(2), E65-E71.

[37] Tuncer, T., Ozyurt, F., Dogan, S. et al., (2021). "A novel Covid-19 and pneumonia classification method based on F-transform", *Chemometrics and Intelligent Laboratory Systems*, 210, 104256.